Toxicology Letters 2019; 302: 18-27 (DOI: 10.1016/j.toxlet.2018.11.009)

Title:

Organic chemicals from diesel exhaust particles affects intracellular calcium, inflammation and β-adrenoceptors in endothelial cells

Running title:

DEP-OC affects calcium, inflammation and βARs in endothelial cells

Authors:

Bendik C. Brinchmann [1, 2§], Eric Le Ferrec[3], Normand Podechard[3], Dominique Lagadic-Gossmann[3], Jørn A. Holme[1] and Johan Øvrevik[1§].

Affiliation:

[1]*Department of Air Pollution and Noise, Division of Infection Control and Environmental Health, Norwegian Institute of Public Health, Oslo, Norway.*

[2]*Division of Laboratory Medicine, Faculty of Medicine, University of Oslo, Oslo, Norway.*

[3]*Univ Rennes, Inserm, EHESP, Irset (Institut de recherche en santé, environnement et travail) - UMR_S 1085, F-35000 Rennes, France*

[§]Corresponding authors: Bendik C. Brinchmann; E-mail: bendikbrinchmann@gmail.com; Phone: +47 46743632 and Johan Øvrevik, Department of Air Pollution and Noise, Division of Infection Control and Environmental Health, Norwegian Institute of Public Health. PO Box 4404 Nydalen, N-0403 Oslo, Norway. E-mail: Johan.Ovrevik@fhi.no; Phone: +47 21076408

Keywords: diesel exhaust particles, extractable organic material, endothelial dysfunction, calcium signalling, beta adrenoceptors, protease activated receptor.

Abstract

Exposure to diesel exhaust particles (DEP) may contribute to endothelial dysfunction and cardiovascular disease. DEP, extractable organic material from DEP (DEP-EOM) and certain PAHs seem to trigger $[Ca^{2+}]_i$ increase as well as inflammation *via* GPCRs like βARs and PAR-2. In the present study we explored the involvement of βARs and PAR-2 in effects of DEP-EOM on $[Ca^{2+}]_i$ and expression of inflammation-associated genes in the endothelial cell-line HMEC-1. We exposed the human microvascular endothelial cell line HMEC-1 to DEP-EOM fractionated by sequential extraction with solvents of increasing polarity: *n*-hexane (*n*-Hex-EOM), dichloromethane (DCM-EOM), methanol (Methanol-EOM) and water (Water-EOM). While Methanol-EOM and Water-EOM had no marked effects, *n*-Hex-EOM and DCM-EOM enhanced $[Ca^{2+}]_i$ (2-3 times baseline) and expression of inflammation-associated genes (IL-1α, IL-1β, COX-2 and CXCL8; 2-15 times baseline) in HMEC-1. The expression of βARs (60-80% of baseline) and βAR-inhibitor carazolol suppressed the increase in $[Ca^{2+}]_i$ induced by both *n*-Hex- and DCM-EOM. Carazolol as well as the Ca^{2+}-channel inhibitor SKF-96365 reduced the DCM-EOM-induced pro-inflammatory gene-expression. Overexpression of βARs increased DCM-EOM-induced $[Ca^{2+}]_i$ responses in HEK293 cells, while βAR-overexpression suppressed $[Ca^{2+}]_i$ responses from *n*-Hex-EOM. Furthermore, the PAR-2-inhibitor ENMD-1068 attenuated $[Ca^{2+}]_i$ responses to DCM-EOM, but not *n*-Hex-EOM in HMEC-1.

The results suggest that βAR and PAR-2 are partially involved in effects of complex mixtures of chemicals extracted from DEP on calcium signalling and inflammation-associated genes in the HMEC-1 endothelial cell-line.

Abbrevetaions: aryl hydrocarbon receptor (AhR), β-adrenoceptors (βAR), benzo[*a*]pyrene (B[*a*]P), calcium (Ca^{2+}), cardiovascular disease (CVD), DEP extracted by: *n*-hexane (*n*-Hex-EOM), dichloromethane (DCM-EOM), methanol (Methanol-EOM), water at 25 °C (Water-EOM), diesel exhaust particles (DEP), endothelial nitric oxide synthase (eNOS), extractable organic material of DEP (DEP-EOM), human microvascular endothelial cell-line (HMEC-1), human embryonic kidney cells (HEK293), wild type (WT), intracellular calcium concentrations ($[Ca^{2+}]_i$), inositol trisphosphate (IP3), G-protein coupled receptors (GPCR), particulate matter (PM), protease-activated receptor-2 (PAR-2), polycyclic aromatic hydrocarbons (PAHs), nuclear factor-κB (NF-κB), 1-nitro-pyrene (1-NP), dimethyl sulfoxide (DMSO), cyclooxygenase 2 (COX-2), interleukin 8 (CXCL8), matrix metalloproteinase 1 (MMP-1)

1. Introduction

Air pollution especially particulate matter (PM), is one of the leading environmental causes of cardiovascular disease (CVD) (Brook et al., 2010; HEI, 2017). PM seems to contribute to CVD and progression of atherosclerosis *via* endothelial dysfunction (Donaldson et al., 2001; Moller et al., 2011), defined as an alteration of endothelial cells towards a pro-inflammatory and pro-constrictive phenotype (Dharmashankar and Widlansky, 2010; Ramji and Davies, 2015). However, the precise molecular mechanisms involved in this process are still largely unknown.

Diesel exhaust particles (DEP) are major constituents of urban PM and contain complex mixtures of organic chemicals adhered to the surfaces of carbon cores (Cohen A. J. et al., 2004; Grahame et al., 2014; Maricq, 2007). Many biologic effects of DEP have been attributed to soluble organic chemicals such as polycyclic aromatic hydrocarbons (PAHs), quinones and dioxins as well as modified PAHs such as nitro-PAHs (Bonvallot et al., 2001; Brinchmann et al., 2018a; Brinchmann et al., 2018b; Kawasaki et al., 2001; Keebaugh et al., 2015; Totlandsdal et al., 2012). Lipophilic compounds such as PAHs may rapidly diffuse across the alveolar-capillary barrier into the bloodstream and target the vasculature (Brinchmann et al., 2018b; Gerde, 2001; Penn et al., 2005).

Beta-adrenoceptors (βARs) are G-protein-coupled receptors (GPCRs) that transmit signalling from the catecholamine hormones adrenaline and noradrenaline acting as regulators of stress responses (Santos and Spadari-Bratfisch, 2006). While β1- and β2ARs are expressed in the lung, heart, vasculature and peripheral tissues, β3-ADRs are mainly expressed in adipose tissue (Bylund et al., 1994; Lowell and Flier, 1997). The overall role of βAR signalling is to regulate cardiopulmonary function and immune responses, and these receptors are thus among the main drug-targets in CVD treatment (De Backer, 2003; Kolmus et al., 2015; Wachter and Gilbert, 2012). PAHs such as pyrene, benzo[*a*]pyrene (B[*a*]P), benzo[*e*]pyrene and chrysene, as well as 1-nitropyrene (1-NP) known to be present in DEP increase intracellular calcium concentration $[Ca^{2+}]_i$ in the human bronchial epithelial cell-line (BEAS-2B) and human microvascular endothelial cell-line (HMEC-1) (Mayati et al., 2014; Mayati et al., 2012a; Mayati et al., 2012b). β2ARs were involved in effects on $[Ca^{2+}]_i$ triggered by B[*a*]P and 1-NP (Mayati et al., 2014; Mayati et al., 2012b). Furthermore, $[Ca^{2+}]_i$ in endothelial cells regulates blood pressure and flow *via* endothelial nitric oxide synthase (eNOS) and more directly via Ca^{2+}-regulated K^+-channels and myoendothelial microdomains (Moller et al., 2011; Sandow et al., 2009; Sandow et al., 2012). Interestingly, diesel

exhaust exposure seem to impair calcium-dependent vasomotor function in healthy men (Barath et al., 2010; Lucking et al., 2011); an effect that may relate to disturbed endothelial $[Ca^{2+}]_i$.

Inflammatory effects of organic chemicals known to be present on DEP, seem to depend on increased $[Ca^{2+}]_i$ (Mayati et al., 2014; Monteiro et al., 2008; N'Diaye et al., 2006; Zhao et al., 1996). We have previously shown that βARs may be involved in $[Ca^{2+}]_i$ increase and induction of the pro-inflammatory chemokine CXCL8 in human bronchial epithelial BEAS-2B cells exposed to 1-NP, one of the dominating nitro-PAHs in DEP (Mayati et al., 2014). Other GPCRs have also been implicated in DEP-induced Ca^{2+} signaling and inflammation. Extractable organic material of DEP (DEP-EOM) increased $[Ca^{2+}]_i$ *via* protease activated receptor 2 (PAR-2) in primary human bronchial cells (Li et al., 2011). Furthermore, DEP-induced inflammatory responses in BEAS-2B, HMEC-1 and primary endothelial cells seemed at least partly dependent on PAR-2 (Bach et al., 2015; Brinchmann et al., 2018b). PAR activation may promote conversion of endothelial cells into a pro-inflammatory phenotype. In conditions with endothelial dysfunction, PARs also mediate contraction and may thus contribute to atherosclerosis and hypertension (Alberelli and De Candia, 2014).

DEP and DEP-EOM have been shown to induce calcium signalling, and pro-inflammatory responses in endothelial cells (Brinchmann et al., 2018a; Brinchmann et al., 2018b; Lawal et al., 2015; Yin et al., 2013). Furthermore, GPCRs seem to be involved in calcium responses and activation of pro-inflammatory responses induced by organic chemicals known to be presents in DEP (Brinchmann et al., 2018a; Brinchmann et al., 2018b; Li et al., 2011; Mayati et al., 2014; Mayati et al., 2012b). Based on this, we explored the hypothesis that βARs and PAR-2, are involved in effects of DEP-EOM on $[Ca^{2+}]_i$ and expression of inflammation-associated genes in the endothelial cell-line HMEC-1.

2. Materials and Methods

2.1. Chemicals

Dimethyl sulfoxide (DMSO) and hydrocortisone purchased from Sigma-Aldrich (St. Louis, MO). L-Glutamine (200 mM) purchased from Thermo Fischer Scientific (Scotland); endothelial growth factor from Nerliens Meszansky (Oslo, Norway); penicillin and streptomycin from Lonza (Walkersville, MD, USA); MCDB 131 medium was provided by Life technologies

(NY, USA); fetal calf serum (FCS) from Biochrom AG (Berlin, Germany). Pluronic acid and fura-2 acetoxymethyl ester (Fura-2-AM) purchased from Invitrogen. Carazolol, 2'-5'-dideoxyadenosine (dd-Ado) and ICI-118,551 from Sigma Aldrich. 1-[2-(4-Methoxyphenyl)-2-[3-(4-methoxyphenyl)propoxy]ethyl-1H-imidazole hydrochloride (SKF 96365) purchased from TOCRIS (Bristol, UK).

2.2. Diesel exhaust particles, chemical extraction and analysis

Diesel exhaust particles (DEP) collected from the tail-pipe of a diesel engine (Deutz, 4 cylinder, 2.2 l, 500 rpm) running on gas oil ; were kindly provided by Flemming R. Cassee (RIVM, the Netherlands). The physicochemical characteristics of this DEP is available elsewhere (Brinchmann et al., 2018b; Totlandsdal et al., 2010; Totlandsdal et al., 2014). To avoid loss of semi-volatile organic compounds, the DEP was stored at -18 °C. Combustion technology has advanced since these particles where collected, but the car-fleet in most cities is still composed of vehicles of differing age and type. These particles where used since they contain a high level (approximately 60%) of organic carbon. DEP-EOM was extracted with a sequence of solvents of increasing polarity ranging from non-polar to polar and chemically characterized as previously described (Brinchmann et al., 2018a; Brinchmann et al., 2018b; Cochran and Kubátová, 2015). In short, DEP-EOM was extracted by sequential pressurized extraction (137 bar) with: *n*-hexane (*n*-Hex-EOM: non-polar), dichloromethane (DCM-EOM: weakly polar) and methanol (Methanol-EOM: semi-polar) at 100°C followed by a final extraction with water at 25°C (Water-EOM: highly polar). The solvents were removed by evaporating the samples to dryness under a gentle stream of nitrogen and extracted DEP-EOM re-suspended in DMSO at concentrations corresponding to extracts from 25 mg/mL of the original DEP.

Chemical composition of *DEP-EOM fractions:* The chemical composition of the four fractionated DEP-EOM fractions have been characterized elsewhere (Brinchmann et al., 2018a; Brinchmann et al., 2018b). In brief, the majority of organic chemicals extracted, where contained in the *n*-Hex- and DCM-EOM fractions. Furthermore, PAHs and aliphatic hydrocarbons, where only retrieved in *n*-Hex- and DCM-EOM. The *n*-Hex-EOM had substantially higher concentrations of PAHs and aliphatic hydrocarbons (respectively 1.5 and 100 mg/g DEP) compared to DCM-EOM (respectively 0.3 and 17.5 mg/g DEP). The dominating PAHs and PAH-derivatives contained in *n*-Hex-EOM were (in rank order): methylated phenanthrenes and/or anthracenes >> phenanthrene > pyrene > methylated fluoranthenes and/or pyrenes > chrysene > 1-nitropyrene > xanthone > fluoranthene > 9-fluorenone. In DCM-EOM the only PAHs found in considerable amounts were (in

rank order): pyrene > phenanthrene ≈ fluoranthrene ≈ chrysene. Methylated, oxidized or nitrated PAH-species were not detected in DCM-EOM (Brinchmann et al., 2018a). Notably, the total amount of organic carbon extracted by n-hexane (153 mg/g DEP), DCM (113 mg/g DEP) and methanol (62 mg/g DEP) decreased according to polarity of the solvents (Brinchmann et al., 2018b). However, organic carbon was much more evenly distributed across these three fractions, compared to PAHs and aliphatic chemicals, which were predominately extracted by *n*-hexane. The reason for this apparent discrepancy, was that the DCM and methanol extracts predominately contained higher molecular weight (MW) compounds which could not be detected by GC-MS since their boiling points were above the ~300°C of the GC-injector (Brinchmann et al., 2018b).

2.3. Cell cultures and treatments

Human microvascular endothelial cell-line (HMEC-1) (LGC Standards, Germany) were maintained in MCDB131 medium containing epidermal growth factor (10 ng/mL), hydrocortisone (0.2 µg/mL), penicillin (50 unit/mL), and streptomycin (50 µg/mL) and supplemented with 10% fetal calf serum (FCS), according to the providers instructions.

Human embryonic kidney cells (HEK293) were maintained in Dulbecco's modified Eagle's medium, containing penicillin (50 units/mL) and streptomycin (50 µg/mL) and supplemented with 10% FCS. HEK293 permanently expressing β1- and β2ARenergic receptors (β1AR, β2AR) were obtained by β1AR, β2AR cDNA transfection as previously described (Mayati et al., 2012b). Briefly, HEK293 were seeded at $2.5x10^5$ cells/well in 6-well plates, transfected with either 2.5 µg of empty pcDNA3.1(+)neo vector (HEKwt) or 2.5 µg of pcDNA3.1(+)neo vector containing HA-tagged human β1AR or β2AR ORF (HEK β1 and HEK β2), and subsequently selected with G418 sulfate (1 mg/mL).

Chemicals were prepared as stock solution in DMSO. The final concentration of solvent did not exceed 0.2% (v/v); control cultures received similar concentration of DMSO. In all experiments with chemical inhibitors, cells were pre-treated 30 min prior to and during exposure.

2.4. Calcium measurements

Variations in intracellular Ca^{2+} concentrations ($[Ca^{2+}]_i$) were analysed in HMEC-1 and HEK293 exposed to DEP-EOM, by micro-spectrofluorometry using the Ca^{2+} sensitive probe Fura-2AM, as previously reported (Brinchmann et al., 2018a). Briefly, cells were incubated at 37 °C in cell suspension buffer (134.8 mM NaCl, 4.7 mM KCl, 1.2 mM K_2HPO_4 , 1 mM $MgCl_2$, 1 mM $CaCl_2$, 10 mM glucose, 10 mM HEPES, pH 7.4) supplemented with 1.5 µM Fura-2AM and 0.006%

pluronic acid. After 30 min loading, cells were washed two times with the buffer before exposure. DEP-EOM corresponding to 5 µg/mL of original DEP was added to the buffer as a bolus dose, after 3 minutes of measuring baseline calcium levels. $[Ca^{2+}]_i$ imaging in HMEC-1 exposed to all four DEP-EOM was conducted at 0 and 60 min of exposure. The experimental protocol for $[Ca^{2+}]_i$ imaging in HEK293 and HMEC-1 exposed to *n*-Hex- or DCM-EOM with or without inhibitors, involved data acquisition every 10th second (emission at 510 nm) at 340- and 380-nm excitation wavelengths. Changes in $[Ca^{2+}]_i$ were monitored using a DMIRB (Leica, Wetzlar, Germany) inverted microscope-based imaging system equipped with a 40×/1.35 UApo N340 high UV light transmittance oil immersion objective (Olympus, Waltham, MA, USA), a CoolSnapHQ fast-cooled monochromatic digital camera (Princeton instrument), a DG-4 Ultra High Speed Wavelength Switcher (Sutter Instruments, Novato, CA, USA) for fluorophore excitation, and METAFLUOR software (Universal Imaging, Downingtown, PA, USA) for image acquisition and analysis.. Analysis involved determination of pixels assigned to each cell. The average pixel value allocated to each cell was obtained with excitation at each wavelength and corrected for background. The ratio was obtained after dividing the 340-nm by the 380-nm fluorescence image on a pixel-by-pixel base (R=F340 nm/F380 nm). Results are presented as normalized calcium level compared to basal $[Ca^{2+}]_i$ measured 3 min prior to exposure. Area under the curve (AUC) was calculated from baseline (1.0).

2.5. Gene expression analysis by real-time qPCR

HMEC-1 destined for q-PCR were grown to near-confluency and serum starved for a minimum of 12 h prior to exposure. Cells were then exposed by removing the media and adding growth medium without FCS containing the various DEP-EOM (*n*-Hex-, DCM-, Methanol- or Water-EOM) or DMSO. Exposure concentrations corresponded to 5 or 50 µg/mL of original DEP. After 5 or 24 h exposure, cells were harvested and mRNA isolated. Total RNA was isolated using NucleoSpin RNA Plus (Macherey-Nagel; Düren, Germany) and reverse transcribed to cDNA on a PCR System 2400 (PerkinElmer, Waltham, MA, USA) using a High Capacity cDNA Archive Kit (Applied Biosystems, Foster City, CA, USA). Real-time qPCR was performed using pre-designed TaqMan Gene Expression Assays and TaqMan Universal PCR Master Mix and run on Applied Biosystems 7500 fast software (Applied Biosystems, Foster City, CA, USA). Gene expression of induced IL-1α (Hs00174092_m1), IL-1β (Hs01555410_m1), CXCL8 (Hs00174103_m1), COX-2 (Hs00153133_m1), MMP-1 (Hs00899658_m1), HO-1(Hs01110250_m1), PAI-2/SERPINB2 (Hs01010736_m1), β1AR (Hs02330048_s1) and β2AR (Hs00240532_s1) were normalized against

GAPDH (Hs02758991_g1), and expressed as fold change compared to untreated control as calculated by the ΔΔCt method (ΔCt = Ct[Gene of Interest] – Ct[GAPDH]; ΔΔCt = ΔCt[Treated] – ΔCt[Control]; Fold change = 2[-ΔΔCt]).

2.6. Statistical analysis

Statistical analysis was performed by ANOVA with Holm-Sidak post-test for multiple comparisons. As ANOVA cannot be performed on normalized data, gene expressions were analyzed using the deltaCT-values from the q-PCR measurements. Effects on $[Ca^{2+}]_i$ were quantified as area under the curve (AUC) and statistical comparison conducted with non-parametric t-tests. All calculations were performed using GraphPad Prism 7 software (GraphPad Software, Inc., San Diego, CA).

3. Results:

3.1 Effects of DEP-EOM on $[Ca^{2+}]_i$ and the involvement of βAR signalling.

Cells were first exposed to DEP-EOM fractioned by sequential extraction with solvents of increasing polarity, *n*-Hex-, DCM-, Methanol- and Water-EOM, at concentrations corresponding to 5 µg/mL of the original DEP. $[Ca^{2+}]_i$ was measured prior to exposure and after 1 h. In corroboration with our previous observations (Brinchmann et al., 2018a), exposure to *n*-Hex-EOM and DCM-EOM caused a marked (2 fold) $[Ca^{2+}]_i$ increase (Fig. 1), compared to baseline levels measured prior to exposure. The fractions extracted by the two more polar solvents, Methanol- and Water-EOM, had negligible effects on $[Ca^{2+}]_i$ in HMEC-1 (Fig. 1). To explore if *n*-Hex- and DCM-EOM increased $[Ca^{2+}]_i$ via βAR signalling, we used the potent and unselective βAR-antagonist carazolol (Innis et al., 1979). Cells were pre-treated with carazolol (10 µM) or DMSO, and exposed 1 h to *n*-Hex- or DCM-EOM at concentrations corresponding to extracts from 5 µg/mL of original DEP. Carazolol caused a marked reduction of $[Ca^{2+}]_i$ triggered by both *n*-Hex- and DCM-EOM in HMEC-1 (Fig. 2). While the overall suppressive effects of carazolol $[Ca^{2+}]_i$ was only slightly larger on DCM-EOM compared to *n*-Hex-EOM (as evident from the AUC estimates), DCM-EOM induced $[Ca^{2+}]_i$ was considerably more affected at the later time points. After 60 min exposure, carazolol treatment caused almost 70% reduction in DCM-EOM-induced $[Ca^{2+}]_i$ increase, whereas *n*-Hex-EOM induced $[Ca^{2+}]_i$ was only suppressed by approximately 40%. Gene-expression analysis of HMEC-1 exposed to the various DEP-EOM indicated that compounds in *n*-Hex- and DCM-EOM resulted in a downregulation of βAR after 24 h exposure (Fig. 3). In line with our

248 previous report on B[*a*]P (Mayati et al., 2017), this indicates that lipophilic organic chemicals
249 extracted by the two least polar solvents interacts with and desensitizes βARs. In contrast, the
250 hydrophilic extracts had no significant effects.
251 To further study the link between βAR and increased $[Ca^{2+}]_i$ we explored effects of *n*-
252 Hex- and DCM-EOM in HEK293 cells, known to express little or no βAR. HEK293 wild type cells
253 (HEK WT) and HEK293 cells over-expressing β1AR (HEK β1) or β2AR (HEK β2) were then
254 exposed to *n*-Hex- or DMC-EOM (5 µg/mL) and $[Ca^{2+}]_i$ measured. It seemed that *n*-Hex-EOM
255 increased $[Ca^{2+}]_i$ via other receptors than βARs in HEK293, as $[Ca^{2+}]_i$ was increased substantially
256 in HEK WT (Fig. 4A). Notably, over-expression of βAR rather had a negative effect on *n*-Hex-
257 EOM triggered $[Ca^{2+}]_i$ increase. DCM-EOM on the other hand, only marginally affected $[Ca^{2+}]_i$ in
258 HEK WT, and $[Ca^{2+}]_i$-responses were considerably stronger in HEK293 overexpressing β1- or
259 β2AR (Fig. 4B). Thus, DCM-EOM seemed to increase $[Ca^{2+}]_i$ via βAR signalling in HEK293 as
260 well as HMEC-1. To further clarify the role of βAR in mediating DCM-EOM-triggered calcium we
261 used the more β2-selective inhibitor ICI-118,551, that reduced $[Ca^{2+}]_i$ in HMEC-1 indicating a
262 possible role of β2AR (Supplementary Fig. S1).
263 PAR-2 is an important mediator of endothelial dysfunction (Alberelli and De Candia,
264 2014). We have previously shown that PAR-2 is involved in mediating the inflammatory responses
265 triggered by *n*-Hex- and DCM-EOM in HMEC-1 and primary human endothelial cells (Brinchmann
266 et al., 2018b). We thus wanted to explore the role of PAR2in calcium effects of *n*-Hex and DCM-
267 EOM. The inhibitor ENMD-1068 (2.5 mM) did not affect *n*-Hex-EOM-induced $[Ca^{2+}]_i$ increase
268 (Fig 5A), but effects of DCM-EOM was reduced by ENMD-1068 treatment (Fig. 5B).
269

270 ### 3.2. Effects of lipophilic DEP-EOM on inflammation-associated genes, involvement of
271 ### βARs and $[Ca^{2+}]_i$.

272 In a recent study on the currently used DEP-EOM, we found that *n*-Hex- and DCM-
273 EOM affected inflammation-associated genes in HMEC-1 and primary endothelial cells
274 (Brinchmann et al., 2018b). In agreement with the current results on $[Ca^{2+}]_i$ and βAR expression,
275 the hydrophilic extracts, methanol-EOM and water-EOM had little or no effect on inflammation-
276 associated genes. To explore the role of βARs with regard to expression of genes linked to
277 inflammation, we pre-treated HMEC-1 with the βAR-antagonist carazolol, prior to exposure to *n*-
278 Hex- and DCM-EOM at a concentration corresponding to 50 µg/mL of original DEP. Carazolol did
279 not inhibit the *n*-Hex-EOM-induced gene-expression (Fig 6A), but somewhat surprisingly

augmented expression of IL-1α (from 5 fold to 8 fold). By contrast, in HMEC-1 exposed to DCM-EOM carazolol suppressed the up-regulation of COX-2 primarily, and to a certain extent CXCL8 and MMP-1(Fig. 6B). Induction of MMP-1 was small and effects on CXCL8 were variable, thus these effects should be interpreted with caution.

In an attempt to further link inflammatory effects to $[Ca^{2+}]_i$, we applied SKF 96365, an inhibitor of transient receptor potential (TRP) channels. We previously found that SKF 96365 reduced effects of DCM-EOM and to a lesser degree *n*-Hex-EOM on $[Ca^{2+}]_i$ (Brinchmann et al., 2018a). HMEC-1 pre-treated with SKF 96365 or DMSO, were exposed 5 h to *n*-Hex- or DCM-EOM (50 µg/mL). None of the inflammation-associated genes induced by *n*-Hex-EOM were significantly affected by SKF 96365 (Fig. 7A), while DCM-EOM-induced COX-2 was markedly reduced (Fig. 7B).

4. Discussion:

The intracellular second messenger calcium is kept at a low cytoplasmic concentration in resting cells (Clapham, 2007). Furthermore, inflammatory effects of xenobiotics known to be present on DEP often seem to depend on $[Ca^{2+}]_i$ (Monteiro et al., 2008; N'Diaye et al., 2006; Ovrevik et al., 2017). Recent studies suggest that some PAHs and DEP may trigger $[Ca^{2+}]_i$ increase as well as inflammation *via* GPCRs like βARs and PAR-2 (Bach et al., 2015; Li et al., 2011; Mayati et al., 2014; Mayati et al., 2012b). Notably, effects of DEP on $[Ca^{2+}]_i$ and MMP-1 seemed to be due to lipophilic EOMs in bronchial cells (Li et al., 2011). In line with this, we previously found that lipophilic DEP-EOM triggered pro-inflammatory responses and disrupted $[Ca^{2+}]_i$ *via* AhR nongenomic signalling in endothelial cells (Brinchmann et al., 2018a; Brinchmann et al., 2018b). In the current study we investigated the role of the GPCRs βAR and PAR-2 in these effects and the role of $[Ca^{2+}]_i$ increase in the pro-inflammatory effects of DEP-EOMs. We found that *n*-Hex- and DCM-EOM in contrast to the more polar DEP-EOM increased $[Ca^{2+}]_i$ in HMEC-1, and that these effects partly depended on βARs. Furthermore, some of the inflammation associated genes induced by DCM-EOM seemed to depend on βARs, and effects on $[Ca^{2+}]_i$ and COX-2 seemed partly interconnected.

Effects of PM depends on various physicochemical properties, implying that PM and its constituents may trigger toxic responses via multiple mechanisms (Lewtas, 2007; Longhin et al., 2016; Ovrevik et al., 2017). While the larger particles (PM_{10}) are associated with lung damage, the

311 smaller particles ($PM_{2,5}$) have been especially connected to CVD (Alfaro-Moreno et al., 2007;
312 Brook et al., 2010). Interestingly, ultrafine particles with even more pro-atherogenic potential than
313 $PM_{2,5}$, contained twice as much organic chemicals (Araujo et al., 2008). Furthermore, particulates
314 denuded of organic chemicals lost their atherogenic potential (Keebaugh et al., 2015). Thus, it
315 seems that organic chemicals may be crucial in vascular effects caused by combustion particles.
316 Based on this we chose a DEP sample with a high organic content.
317 We have previously fund that DEP-EOM increased $[Ca^{2+}]_i$ in HMEC-1 at non-
318 cytotoxic concentrations, and the induced changes were at least partly reversible at concentrations
319 currently used (5 µg/mL) (Brinchmann et al., 2018a; Brinchmann et al., 2018b). More specifically,
320 *n*-Hex-EOM appeared to trigger store operated calcium entry (SOCE), while DCM-EOM activated
321 a $[Ca^{2+}]_i$ response resembling receptor-operated calcium entry (ROCE), that seemed totally
322 dependent on extracellular calcium, in HMEC-1. Both effects seemed largely dependent on AhR
323 nongenomic signalling (Brinchmann et al., 2018a). Chemical analysis of these DEP-extracts
324 showed marked differences in chemical composition. While *n*-Hex-EOM contained a multitude of
325 PAHs, we only detected considerable amounts of phenanthrene, fluoranthene, pyrene and chrysene
326 in DCM-EOM. Ongoing studies have revealed that it is difficult to estimate calcium responses from
327 chemical composition in complex mixtures, as B[*a*]P attenuated pyrene-induced $[Ca^{2+}]_i$ increase
328 (Brinchmann et al submitted). Thus, the marked differences in $[Ca^{2+}]_i$ response patterns induced by
329 the two DEP-EOM fractions (SOCE *vs* ROCE) may indeed relate to differences in chemical
330 composition, more specifically a changed balance between specific PAHs. However, the total
331 amount of organic chemicals was higher in *n*-Hex- (~150 mg/g of original DEP) compared to
332 DCM-EOM (~110 mg/g), and *n*-Hex-EOM contained approximately 5-fold more PAHs and 7-fold
333 more aliphatic compounds (Brinchmann et al., 2018a). Furthermore, we have found that *n*-Hex-
334 EOM increased $[Ca^{2+}]_i$ at considerably lower concentrations than DCM-EOM (Brinchmann et al.,
335 2018a). Thus, we cannot exclude the possibility that discrepancies in $[Ca^{2+}]_i$ response patterns may
336 just relate to higher concentrations of organic compounds in *n*-Hex-EOM.
337 The most robust finding of the present study is that βARs were involved in effects of
338 DCM-EOM on $[Ca^{2+}]_i$ in both HMEC-1 and HEK293. Compared to HMEC-1, βARs are poorly
339 expressed in HEK293 WT cells (Mayati et al., 2012b; von Zastrow and Kobilka, 1992). In line with
340 this, DCM-EOM induced only marginal $[Ca^{2+}]_i$ responses in HEK293 WT cells, but this response
341 was substantially increased in HEK293 over-expressing β1- or β2AR. This thus indicates that βARs
342 mediated-effects of chemicals present in DCM-EOM may not be restricted by cell type.

Acknowledging that these lipophilic DEP-EOM affect multiple mechanisms, it is tempting to speculate that DCM-EOM activates ROCE *via* the GPCRs βAR and PAR-2. Studies indicating that certain PAHs may act as βAR agonists and that DEP increase $[Ca^{2+}]_i$ *via* PAR-2 in human bronchial cells, lend support to this suggestion (Li et al., 2011; Mayati et al., 2014; Mayati et al., 2012b; Mayati et al., 2017). However, as we have previously observed that DCM-EOM increased $[Ca^{2+}]_i$ via AhR-dependent mechanisms, the possibility that GPCRs could be trans-activated downstream of AhR activation also needs to be considered.

Notably, AhR-nongenomic signalling appears to be the main triggering mechanism for both the *n*-Hex- and DCM-EOM induced $[Ca^{2+}]_i$-increase in HMEC-1 (Brinchmann et al., 2018a). While the carazolol-effect suggests that βARs also contributed to *n*-Hex-EOM-induced $[Ca^{2+}]_i$-increase in HMEC-1, the results obtained in HEK293 appeared quite contradictory. In HEK293 WT, which constitutively express marginal levels of βAR (von Zastrow and Kobilka, 1992), *n*-Hex-EOM increased $[Ca^{2+}]_i$ markedly, clearly showing that this effect was independent of βARs and triggered *via* other signalling mechanisms. Furthermore, overexpression of β1-/β2AR suppressed *n*-Hex-EOM triggered $[Ca^{2+}]_i$-increase in HEK293, thus strongly suggesting that there also may be negative crosstalk between β1-/β2AR and AhR signalling pathways, in addition to the positive crosstalk previously reported (Brinchmann et al., 2018a). The nature and overall relevance of this apparent interaction between AhR- and βAR-signalling remains to clarify. It should however, be noted that examples from the literature indicate that increase of βAR-signalling may negatively affect other signalling pathways and thus $[Ca^{2+}]_i$. For instance, phosphatidylinositol 4,5-bisphosphate (PIP2)-dependent calcium channels will be negatively affected by βARs ligands that primarily activate phospholipase C (PLC), leading to PIP2 hydrolysis (Putney and Tomita, 2012; Suh and Hille, 2005). As PIP2 positively regulates a wide range of ion channels, a reduction of PIP2-levels through hydrolysis would be expected to reduce Ca^{2+}-influx through these channels (Suh and Hille, 2005).

COX-2 may produce prostaglandin E2, which promotes expression of matrix metalloproteinases (MMPs), tissue destruction, cell death and destabilization of atherosclerotic plaques (Bishop-Bailey et al., 2006; Gomez et al., 2014; Gomez et al., 2013; Newby, 2016; Walton et al., 1999). In bronchial epithelial cells it has been found that lipophilic components of DEP induce MMP-1 via calcium signalling (Li et al., 2011). Thus, a central focus of this study was to explore whether DEP-EOM-induced increases in $[Ca^{2+}]_i$ and gene-expression were interconnected, or rather parallel events. The βAR antagonist carazolol and the calcium antagonist SKF96365, had

little or no effect on *n*-Hex-EOM and most of the genes induced by DCM-EOM where unaffected. Thus, βARs and Ca^{2+}-signalling did not seem to be pivotal in mediating the observed effects on inflammation-associated genes. However, DCM-EOM-induced COX-2 expression was reduced by both carazolol and SKF96365, indicating that Ca^{2+}-signalling is an upstream event at least partly involved in regulation of COX-2. This may be related to protein kinase C (PKC), which is involved in the regulation of COX-2 and is activated by Ca^{2+} and di-acyl-glycerol (DAG) (Mochly-Rosen et al., 2012). Moreover, GPCRs may activate PLC, which is detrimental to $[Ca^{2+}]_i$-regulation (Putney and Tomita, 2012). Thus, a possible chain of events is that certain lipophilic chemicals in DEP may activate GPCRs, directly or indirectly through AhR, subsequently triggering the PLC/DAG/Ca^{2+}/PKC-cascade leading to activation of COX-2 and other pro-inflammatory genes. In contrast, *n*-Hex-EOM-induced gene expression was not affected by neither SKF96365 nor carazolol, despite effects of these inhibitors on *n*-Hex-EOM-induced $[Ca^{2+}]_i$ in HMEC-1. Thus, $[Ca^{2+}]_i$ does not seem central to these responses. However, care should be taken when comparing these findings, as effects on inflammation-associated genes were examined after 5 h exposure to 10-fold higher DEP-EOM-concentrations than those used to study Ca^{2+}-signalling over the first 60 min of exposure.

In conclusion, neither βAR nor PAR-2 were consistently involved in effects of *n*-Hex-EOM in HMEC-1 cells, but both GPCRs seemed at least partly involved in regulation of calcium signalling and COX-2 responses in cells exposed to DCM-EOM. This discrepancy in involvement of GPCRs in cellular effects of DEP-EOM fractionated by solvents of increasing polarity is likely due to differences in chemical composition and/or the amount of active compounds extracted. Thus, βAR and PAR-2, does not appear to play a major role in mediating the observed effects of DEP-EOM on $[Ca^{2+}]_i$ and inflammation-associated genes in HMEC-1, but may conceivably contribute to modulate responses.

Competing interests

The authors report no competing interests. The authors alone are responsible for the content and writing of the paper.

Authors' contributions

BB performed all experiments, and contributed in all experimental planning and design in collaboration with ELF, JØ, DLG and JAH. BB, NP and JØ performed data analysis and statistics. JØ conceived and coordinated the study, with support of JAH, ELF and DLG. BB drafted the first

versions of the manuscript and wrote the final version in collaboration with JØ and JAH. All authors read, commented and approved the final manuscript.

Acknowledgements:

We thank E. Lilleaas (Norwegian Inst. of Public Health, Oslo, Norway) for technical assistance throughout the study, and Alena Kubátová and Klára Kukowski (University of North Dakota, Grand Forks, ND, USA) for preparing and characterizing the DEP-EOM. We thank the microscopy platform at Rennes University, Plateforme IBiSA MRic-Photonics Université de Rennes 1 SFR Biosit (UMS 3480 - US 018). The work was supported by the Research Council of Norway through the Environmental Exposures and Health Outcomes-program (grant no. 228143). We also thank Rennes Métropole (France) for travel exchange grants.

References:

Alberelli, M.A., De Candia, E., 2014. Functional role of protease activated receptors in vascular biology. Vascul Pharmacol 62, 72-81.

Alfaro-Moreno, E., Nawrot, T.S., Nemmar, A., Nemery, B., 2007. Particulate matter in the environment: pulmonary and cardiovascular effects. Current opinion in pulmonary medicine 13, 98-106.

Araujo, J.A., Barajas, B., Kleinman, M., Wang, X., Bennett, B.J., Gong, K.W., Navab, M., Harkema, J., Sioutas, C., Lusis, A.J., Nel, A.E., 2008. Ambient particulate pollutants in the ultrafine range promote early atherosclerosis and systemic oxidative stress. Circ Res 102, 589-596.

Bach, N., Bolling, A.K., Brinchmann, B.C., Totlandsdal, A.I., Skuland, T., Holme, J.A., Lag, M., Schwarze, P.E., Ovrevik, J., 2015. Cytokine responses induced by diesel exhaust particles are suppressed by PAR-2 silencing and antioxidant treatment, and driven by polar and non-polar soluble constituents. Toxicol Lett 238, 72-82.

Barath, S., Mills, N.L., Lundback, M., Tornqvist, H., Lucking, A.J., Langrish, J.P., Soderberg, S., Boman, C., Westerholm, R., Londahl, J., Donaldson, K., Mudway, I.S., Sandstrom, T., Newby, D.E., Blomberg, A., 2010. Impaired vascular function after exposure to diesel exhaust generated at urban transient running conditions. Part Fibre Toxicol 7, 19.

Bishop-Bailey, D., Mitchell, J.A., Warner, T.D., 2006. COX-2 in cardiovascular disease. Arterioscler Thromb Vasc Biol 26, 956-958.

Bonvallot, V., Baeza-Squiban, A., Baulig, A., Brulant, S., Boland, S., Muzeau, F., Barouki, R., Marano, F., 2001. Organic compounds from diesel exhaust particles elicit a proinflammatory response in human airway epithelial cells and induce cytochrome p450 1A1 expression. Am J Respir Cell Mol Biol 25, 515-521.

Brinchmann, B.C., Le Ferrec, E., Podechard, N., Lagadic-Gossmann, D., Shoji, K.F., Penna, A., Kukowski, K., Kubatova, A., Holme, J.A., Ovrevik, J., 2018a. Lipophilic Chemicals from Diesel Exhaust Particles Trigger Calcium Response in Human Endothelial Cells via Aryl Hydrocarbon Receptor Non-Genomic Signalling. International journal of molecular sciences 19.

Brinchmann, B.C., Skuland, T., Rambol, M.H., Szoke, K., Brinchmann, J.E., Gutleb, A.C., Moschini, E., Kubatova, A., Kukowski, K., Le Ferrec, E., Lagadic-Gossmann, D., Schwarze, P.E., Lag, M., Refsnes, M., Ovrevik, J., Holme, J.A., 2018b. Lipophilic components of diesel exhaust particles induce pro-inflammatory responses in human endothelial cells through AhR dependent pathway(s). Part Fibre Toxicol 15, 21.

Brook, R.D., Rajagopalan, S., 2012. Chronic air pollution exposure and endothelial dysfunction: what you can't see--can harm you. J Am Coll Cardiol 60, 2167-2169.

Brook, R.D., Rajagopalan, S., Pope, C.A., 3rd, Brook, J.R., Bhatnagar, A., Diez-Roux, A.V., Holguin, F., Hong, Y., Luepker, R.V., Mittleman, M.A., Peters, A., Siscovick, D., Smith, S.C., Jr., Whitsel, L., Kaufman, J.D., American Heart Association Council on, E., Prevention, C.o.t.K.i.C.D., Council on Nutrition, P.A., Metabolism, 2010. Particulate matter air pollution and cardiovascular disease: An update to the scientific statement from the American Heart Association. Circulation 121, 2331-2378.

Bylund, D.B., Eikenberg, D.C., Hieble, J.P., Langer, S.Z., Lefkowitz, R.J., Minneman, K.P., Molinoff, P.B., Ruffolo, R.R., Jr., Trendelenburg, U., 1994. International Union of Pharmacology nomenclature of adrenoceptors. Pharmacol Rev 46, 121-136.

Campen, M.J., 2012. Vascular endothelium as a target of diesel particulate matter-associated toxicants. Arch Toxicol 86, 517-518.

Clapham, D.E., 2007. Calcium signaling. Cell 131, 1047-1058.

463 Cochran, R.E., Kubátová, A., 2015. Pressurised fluid extraction of polycyclic aromatic
464 hydrocarbons and their polar oxidation products from atmospheric particles. International
465 Journal of Environmental Analytical Chemistry 95, 434-452.
466 Cohen A. J., Anderson H. R., Ostro B., Pandey K. D., Krzyzanowski M., Künzli N., Gutschmidt K,
467 Pope III C. A., Romieu I., Samet J. M., R., S.K., 2004. Urban Air Pollution. In: Ezzati, M., Lopez,
468 A.D., Rodgers, A., Murray, C.J.L. (Eds.) Comparative Quantification of Health Risks - Global and
469 Regional Burden of Diseases Attributable to Selected Major Risk Factors. World Health
470 Organization, World Health Organization.
471 De Backer, G., 2003. European guidelines on cardiovascular disease prevention in clinical
472 practice Third Joint Task Force of European and other Societies on Cardiovascular Disease
473 Prevention in Clinical Practice (constituted by representatives of eight societies and by invited
474 experts). European Heart Journal 24, 1601-1610.
475 Dharmashankar, K., Widlansky, M.E., 2010. Vascular endothelial function and hypertension:
476 insights and directions. Curr Hypertens Rep 12, 448-455.
477 Donaldson, K., Stone, V., Seaton, A., MacNee, W., 2001. Ambient Particle Inhalation and the
478 Cardiovascular System: Potential Mechanisms. Environ Health Perspect.
479 Edwards, M.R., Haas, J., Panettieri, R.A., Jr., Johnson, M., Johnston, S.L., 2007. Corticosteroids
480 and beta2 agonists differentially regulate rhinovirus-induced interleukin-6 via distinct Cis-
481 acting elements. J Biol Chem 282, 15366-15375.
482 Gerde, 2001. The rapid alveolar absorption of diesel soot-adsorbed Benzo[a]Pyrene:
483 bioavailability, metabolism and dosimetry of an inhaled particle-borne carcinogen.
484 Carcinogenesis.
485 Gomez, I., Benyahia, C., Louedec, L., Leseche, G., Jacob, M.P., Longrois, D., Norel, X., 2014.
486 Decreased PGE(2) content reduces MMP-1 activity and consequently increases collagen
487 density in human varicose vein. PLoS One 9, e88021.
488 Gomez, I., Foudi, N., Longrois, D., Norel, X., 2013. The role of prostaglandin E2 in human
489 vascular inflammation. Prostaglandins Leukot Essent Fatty Acids 89, 55-63.
490 Grahame, T.J., Klemm, R., Schlesinger, R.B., 2014. Public health and components of particulate
491 matter: the changing assessment of black carbon. Journal of the Air & Waste Management
492 Association (1995) 64, 620-660.
493 HEI, 2017. STATE OF GLOBAL AiR /2017. Boston, MA:Health Effects Institute and The
494 Institute for Health Metrics and Evaluation.
495 Holden, N.S., Rider, C.F., Bell, M.J., Velayudhan, J., King, E.M., Kaur, M., Salmon, M., Giembycz,
496 M.A., Newton, R., 2010. Enhancement of inflammatory mediator release by beta(2)-
497 adrenoceptor agonists in airway epithelial cells is reversed by glucocorticoid action. Br J
498 Pharmacol 160, 410-420.
499 Innis, R.B., Correa, F.M., Synder, S.H., 1979. Carazolol, an extremely potent beta-adrenergic
500 blocker: binding to beta-receptors in brain membranes. Life Sci 24, 2255-2264.
501 Kawasaki, S., Takizawa, H., Takami, K., Desaki, M., Okazaki, H., Kasama, T., Kobayashi, K.,
502 Yamamoto, K., Nakahara, K., Tanaka, M., Sagai, M., Ohtoshi, T., 2001. Benzene-extracted
503 components are important for the major activity of diesel exhaust particles: effect on
504 interleukin-8 gene expression in human bronchial epithelial cells. Am J Respir Cell Mol Biol
505 24, 419-426.
506 Keebaugh, A.J., Sioutas, C., Pakbin, P., Schauer, J.J., Mendez, L.B., Kleinman, M.T., 2015. Is
507 atherosclerotic disease associated with organic components of ambient fine particles? Sci
508 Total Environ 533, 69-75.

509 Kolmus, K., Tavernier, J., Gerlo, S., 2015. beta2-Adrenergic receptors in immunity and
510 inflammation: stressing NF-kappaB. Brain, behavior, and immunity 45, 297-310.
511 Krishnan, R.M., Adar, S.D., Szpiro, A.A., Jorgensen, N.W., Van Hee, V.C., Barr, R.G., O'Neill, M.S.,
512 Herrington, D.M., Polak, J.F., Kaufman, J.D., 2012. Vascular responses to long- and short-term
513 exposure to fine particulate matter: MESA Air (Multi-Ethnic Study of Atherosclerosis and Air
514 Pollution). J Am Coll Cardiol 60, 2158-2166.
515 Lawal, A.O., Zhang, M., Dittmar, M., Lulla, A., Araujo, J.A., 2015. Heme oxygenase-1 protects
516 endothelial cells from the toxicity of air pollutant chemicals. Toxicol Appl Pharmacol 284,
517 281-291.
518 Le Ferrec, E., Øvrevik, J., 2018. G-protein coupled receptors (GPCR) and environmental
519 exposure. Consequences for cell metabolism using the β-adrenoceptors as example. Current
520 Opinion in Toxicology 8, 14-19.
521 Lewtas, J., 2007. Air pollution combustion emissions: characterization of causative agents and
522 mechanisms associated with cancer, reproductive, and cardiovascular effects. Mutat Res 636,
523 95-133.
524 Li, J., Kanju, P., Patterson, M., Chew, W.L., Cho, S.H., Gilmour, I., Oliver, T., Yasuda, R., Ghio, A.,
525 Simon, S.A., Liedtke, W., 2011. TRPV4-mediated calcium influx into human bronchial epithelia
526 upon exposure to diesel exhaust particles. Environ Health Perspect 119, 784-793.
527 Longhin, E., Gualtieri, M., Capasso, L., Bengalli, R., Mollerup, S., Holme, J.A., Ovrevik, J., Casadei,
528 S., Di Benedetto, C., Parenti, P., Camatini, M., 2016. Physico-chemical properties and biological
529 effects of diesel and biomass particles. Environ Pollut 215, 366-375.
530 Lowell, B.B., Flier, J.S., 1997. Brown adipose tissue, beta 3-adrenergic receptors, and obesity.
531 Annual review of medicine 48, 307-316.
532 Lucking, A.J., Lundback, M., Barath, S.L., Mills, N.L., Sidhu, M.K., Langrish, J.P., Boon, N.A.,
533 Pourazar, J., Badimon, J.J., Gerlofs-Nijland, M.E., Cassee, F.R., Boman, C., Donaldson, K.,
534 Sandstrom, T., Newby, D.E., Blomberg, A., 2011. Particle traps prevent adverse vascular and
535 prothrombotic effects of diesel engine exhaust inhalation in men. Circulation 123, 1721-1728.
536 Maricq, M., 2007. Chemical characterization of particulate emissions from diesel engines: A
537 review. Journal of Aerosol Science 38, 1079-1118.
538 Mayati, A., Le Ferrec, E., Holme, J.A., Fardel, O., Lagadic-Gossmann, D., Ovrevik, J., 2014.
539 Calcium signaling and beta2-adrenergic receptors regulate 1-nitropyrene induced CXCL8
540 responses in BEAS-2B cells. Toxicol In Vitro 28, 1153-1157.
541 Mayati, A., Le Ferrec, E., Lagadic-Gossmann, D., Fardel, O., 2012a. Aryl hydrocarbon receptor-
542 independent up-regulation of intracellular calcium concentration by environmental polycyclic
543 aromatic hydrocarbons in human endothelial HMEC-1 cells. Environ Toxicol 27, 556-562.
544 Mayati, A., Levoin, N., Paris, H., N'Diaye, M., Courtois, A., Uriac, P., Lagadic-Gossmann, D.,
545 Fardel, O., Le Ferrec, E., 2012b. Induction of intracellular calcium concentration by
546 environmental benzo(a)pyrene involves a beta2-adrenergic receptor/adenylyl cyclase/Epac-
547 1/inositol 1,4,5-trisphosphate pathway in endothelial cells. J Biol Chem 287, 4041-4052.
548 Mayati, A., Podechard, N., Rineau, M., Sparfel, L., Lagadic-Gossmann, D., Fardel, O., Ferrec, E.L.,
549 2017. Benzo(a)pyrene triggers desensitization of beta2-adrenergic pathway. Sci Rep 7, 3262.
550 Mochly-Rosen, D., Das, K., Grimes, K.V., 2012. Protein kinase C, an elusive therapeutic target?
551 Nature reviews Drug discovery 11, 937-957.
552 Moller, P., Mikkelsen, L., Vesterdal, L.K., Folkmann, J.K., Forchhammer, L., Roursgaard, M.,
553 Danielsen, P.H., Loft, S., 2011. Hazard identification of particulate matter on vasomotor
554 dysfunction and progression of atherosclerosis. Crit Rev Toxicol 41, 339-368.

555 Monteiro, P., Gilot, D., Le Ferrec, E., Rauch, C., Lagadic-Gossmann, D., Fardel, O., 2008. Dioxin-
556 mediated up-regulation of aryl hydrocarbon receptor target genes is dependent on the
557 calcium/calmodulin/CaMKIalpha pathway. Mol Pharmacol 73, 769-777.
558 N'Diaye, M., Le Ferrec, E., Lagadic-Gossmann, D., Corre, S., Gilot, D., Lecureur, V., Monteiro, P.,
559 Rauch, C., Galibert, M.D., Fardel, O., 2006. Aryl hydrocarbon receptor- and calcium-dependent
560 induction of the chemokine CCL1 by the environmental contaminant benzo[a]pyrene. J Biol
561 Chem 281, 19906-19915.
562 Newby, A.C., 2016. Metalloproteinase production from macrophages - a perfect storm leading
563 to atherosclerotic plaque rupture and myocardial infarction. Experimental physiology 101,
564 1327-1337.
565 Ovrevik, J., Refsnes, M., Holme, J.A., Schwarze, P.E., Lag, M., 2013. Mechanisms of chemokine
566 responses by polycyclic aromatic hydrocarbons in bronchial epithelial cells: sensitization
567 through toll-like receptor-3 priming. Toxicol Lett 219, 125-132.
568 Ovrevik, J., Refsnes, M., Lag, M., Brinchmann, B.C., Schwarze, P.E., Holme, J.A., 2017. Triggering
569 Mechanisms and Inflammatory Effects of Combustion Exhaust Particles with Implication for
570 Carcinogenesis. Basic & clinical pharmacology & toxicology 121 Suppl 3, 55-62.
571 Penn, A., Murphy, G., Barker, S., Henk, W., Penn, L., 2005. Combustion-Derived Ultrafine
572 Particles Transport Organic Toxicants to Target Respiratory Cells. Environmental Health
573 Perspectives 113, 956-963.
574 Putney, J.W., Tomita, T., 2012. Phospholipase C signaling and calcium influx. Advances in
575 biological regulation 52, 152-164.
576 Ramji, D.P., Davies, T.S., 2015. Cytokines in atherosclerosis: Key players in all stages of disease
577 and promising therapeutic targets. Cytokine Growth Factor Rev 26, 673-685.
578 Sandow, S.L., Haddock, R.E., Hill, C.E., Chadha, P.S., Kerr, P.M., Welsh, D.G., Plane, F., 2009.
579 What's where and why at a vascular myoendothelial microdomain signalling complex. Clin
580 Exp Pharmacol Physiol 36, 67-76.
581 Sandow, S.L., Senadheera, S., Grayson, T.H., Welsh, D.G., Murphy, T.V., 2012. Calcium and
582 endothelium-mediated vasodilator signaling. Adv Exp Med Biol 740, 811-831.
583 Santos, I.N., Spadari-Bratfisch, R.C., 2006. Stress and cardiac beta adrenoceptors. Stress
584 (Amsterdam, Netherlands) 9, 69-84.
585 Suh, B.C., Hille, B., 2005. Regulation of ion channels by phosphatidylinositol 4,5-bisphosphate.
586 Current opinion in neurobiology 15, 370-378.
587 Totlandsdal, A.I., Cassee, F.R., Schwarze, P., Refsnes, M., Lag, M., 2010. Diesel exhaust particles
588 induce CYP1A1 and pro-inflammatory responses via differential pathways in human
589 bronchial epithelial cells. Part Fibre Toxicol 7, 41.
590 Totlandsdal, A.I., Herseth, J.I., Bolling, A.K., Kubatova, A., Braun, A., Cochran, R.E., Refsnes, M.,
591 Ovrevik, J., Lag, M., 2012. Differential effects of the particle core and organic extract of diesel
592 exhaust particles. Toxicol Lett 208, 262-268.
593 Totlandsdal, A.I., Ovrevik, J., Cochran, R.E., Herseth, J.I., Bolling, A.K., Lag, M., Schwarze, P.,
594 Lilleaas, E., Holme, J.A., Kubatova, A., 2014. The occurrence of polycyclic aromatic
595 hydrocarbons and their derivatives and the proinflammatory potential of fractionated
596 extracts of diesel exhaust and wood smoke particles. J Environ Sci Health A Tox Hazard Subst
597 Environ Eng 49, 383-396.
598 von Zastrow, M., Kobilka, B.K., 1992. Ligand-regulated internalization and recycling of human
599 beta 2-adrenergic receptors between the plasma membrane and endosomes containing
600 transferrin receptors. J Biol Chem 267, 3530-3538.

601 Wachter, S.B., Gilbert, E.M., 2012. Beta-adrenergic receptors, from their discovery and
602 characterization through their manipulation to beneficial clinical application. Cardiology 122,
603 104-112.
604 Walton, L.J., Franklin, I.J., Bayston, T., Brown, L.C., Greenhalgh, R.M., Taylor, G.W., Powell, J.T.,
605 1999. Inhibition of prostaglandin E2 synthesis in abdominal aortic aneurysms: implications
606 for smooth muscle cell viability, inflammatory processes, and the expansion of abdominal
607 aortic aneurysms. Circulation 100, 48-54.
608 Yin, F., Ramanathan, G., Zhang, M., Araujo, J.A., 2013. Prooxidative effects of ambient pollutant
609 chemicals are inhibited by HDL. Journal of biochemical and molecular toxicology 27, 172-183.
610 Zhao, M., Lytton, J., Burchiel, S.W., 1996. Inhibition of sarco-endoplasmic reticulum calcium
611 ATPases (SERCA) by polycyclic aromatic hydrocarbons: lack of evidence for direct effects on
612 cloned rat enzymes. International journal of immunopharmacology 18, 589-598.
613 Øvrevik, J., Arlt, V.M., Øya, E., Nagy, E., Mollerup, S., Phillips, D.H., Låg, M., Holme, J.A., 2010.
614 Differential effects of nitro-PAHs and amino-PAHs on cytokine and chemokine responses in
615 human bronchial epithelial BEAS-2B cells. Toxicology and Applied Pharmacology 242, 270-
616 280.
617
618

Figure legends:

FIGURE 1. **Effects of DEP-EOM on $[Ca^{2+}]_i$ in HMEC-1 cell-line.** A: Cells plated on glass lamellas were loaded with the Ca^{2+}-sensitive probe Fura2-AM and then exposed to DEP-EOM (corresponding to 5 µg DEP/mL). $[Ca^{2+}]_i$ level measured by normalized ratio of the Fura2-AM probe before exposure and after 60 min is presented. B: HMEC-1 cells exposed to the four DEP-extracts: *n*-Hex- (i), DCM- (ii), Methanol- (iii) and Water-EOM (iv) are visualized as presented. Results are expressed as mean ± SEM; n-Hex-EOM and DCM-EOM: n=3; Methanol- and Water-EOM: n=2). *Statistically significant different from baseline.

FIGURE 2. **Effects of the βAR antagonist carazolol on *n*-Hex- and DCM-EOM triggered $[Ca^{2+}]_i$ in HMEC-1.** Cells were pre-treated with the unselective βAR antagonist carazolol (10 µM) or vehicle (DMSO) 30 min prior to exposure. Three min after measurements were started, cells were exposed to *n*-Hex- or DCM-EOM (5 µg/mL). $[Ca^{2+}]_i$ level measured by normalized ratio of the Fura2-AM probe during exposure is presented as graph and the area under the curve (AUC) 0-60 min, as mean and mean ± SEM (n=3). *Statistically significant different from no inhibitor.

FIGURE 3. **DEP-EOM affects βAR expression in HMEC-1.** Cells were exposed to DEP-EOM (5 and 50 µg/mL) ranging from lipophilic to hydrophilic, *n*-Hexane, DCM-, Methanol-, Water-EOM or vehicle (DMSO) alone. The expression of ADRβ1 and ADRβ2 was measured by q-PCR after 2 and 24 h. The m-RNA levels are relative to DMSO, represented by the dotted line at 1. Results are expressed as mean ± SEM (n=4). *Statistically significant different from unexposed controls.

FIGURE 4. **Effects of DEP-EOM on $[Ca^{2+}]_i$ in HEK293 WT, β1 and β2.** A: Three min after measurements were started, HEK WT or HEK cells over expressing β1AR or β2AR were exposed to *n*-Hex- or DCM-EOM (5 µg/mL). $[Ca^{2+}]_i$ level measured by normalized ratio of the Fura2-AM probe during exposure is presented as graph and AUC 0-60 min, as mean and mean ± SEM (n=3). $^{\#}$ and *statistically significant different from HEK WT.

FIGURE 5. **Inhibition of PAR-2 and $[Ca^{2+}]_i$ increased by *n*-Hex- and DCM-EOM in HMEC-1.** Cells were incubated in buffer with or without the PAR-2 inhibitor ENMD-1068 (2.5 mM) 30 min prior to exposure. Three min after measurements were started, the cells were exposed to *n*-Hex- or DCM-EOM at concentrations corresponding to 5 µg/mL of the original DEP or vehicle control

(DMSO). $[Ca^{2+}]_i$ level measured by normalized ratio of the Fura2-AM probe during exposure is presented as graph and the area under the curve (AUC) 0-45 min, as mean and mean ± SEM (*n*-Hex-EOM: n=1; DCM-EOM: n=3), respectively. *Significantly different from no inhibitor.

FIGURE 6. **Effects of carazolol on *n*-Hex- and DCM-EOM induced genes in HMEC-1.** Cells were pre-treated with carazolol (10 μM) 30 min and exposed to 50 μg/mL of the lipophilic fractions, *n*-Hex- (A) or DCM-EOM (B), or vehicle (DMSO). Gene expression measured after 5 h by q-PCR. The m-RNA levels are expressed relative to DMSO, represented by the dotted line at 1. The results are expressed as mean ± SEM (n=3). *Statistically significant difference from unexposed controls. #Statistically significant difference from cells exposed to DEP-EOM without inhibitor.

FIGURE 7. **Effects of the calcium channel inhibitor SKF 96365 on *n*-Hex- and DCM-EOM induced genes in HMEC-1.** Cells were pre-treated with SKF96365 (10 μM) 30 min and exposed to 50 μg/mL of the lipophilic fractions, *n*-Hex- (A) or DCM-EOM (B), or vehicle (DMSO). Gene expression measured after 5 h by q-PCR. The m-RNA levels are expressed relative to DMSO, represented by the dotted line at 1. The results are expressed as mean ± SEM (n=3). *Statistically significant difference from unexposed controls. #Statistically significant difference from cells exposed to DEP-EOM without inhibitor.

671 Figures:

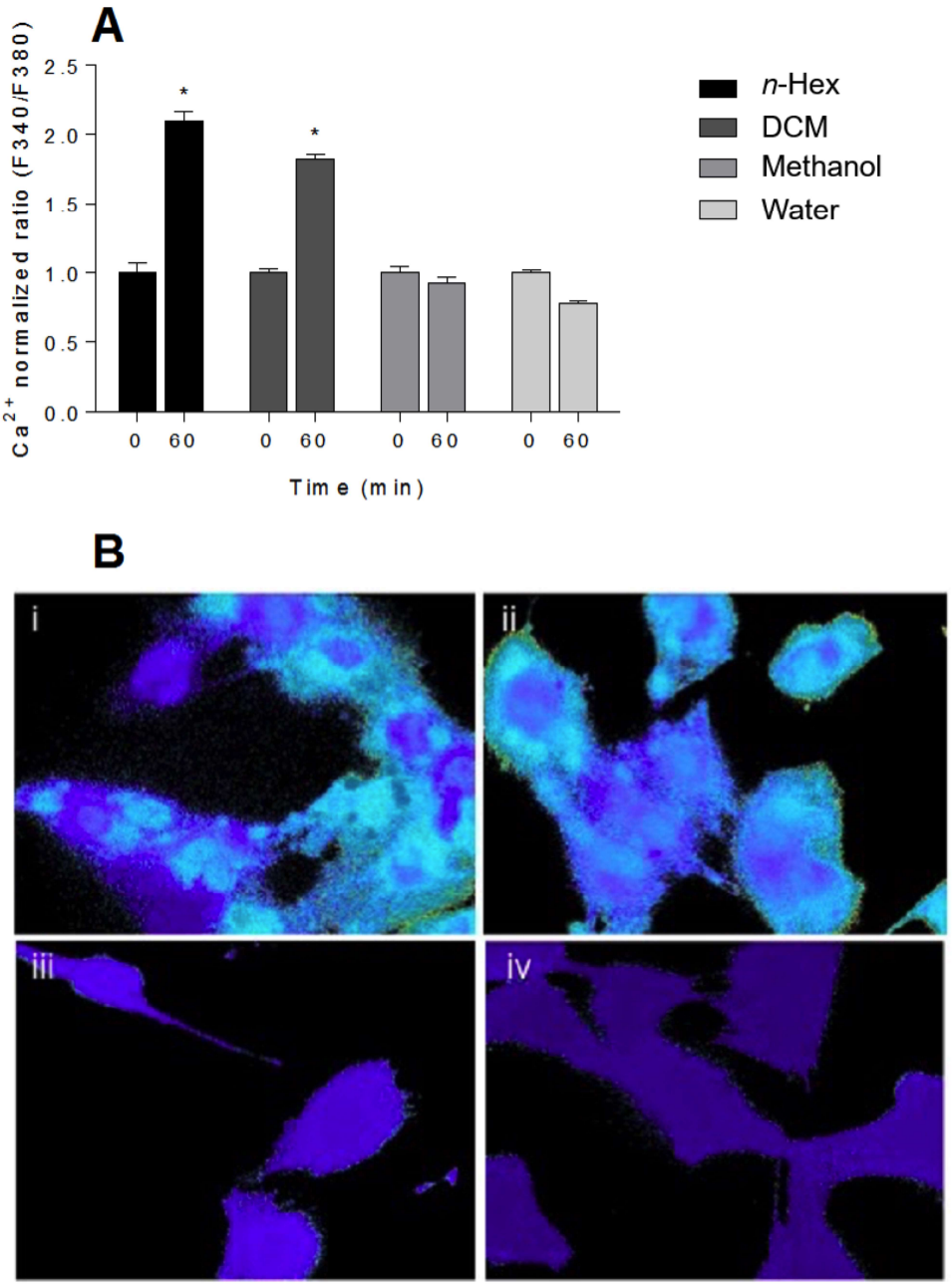

672

673 FIGURE 1.

674

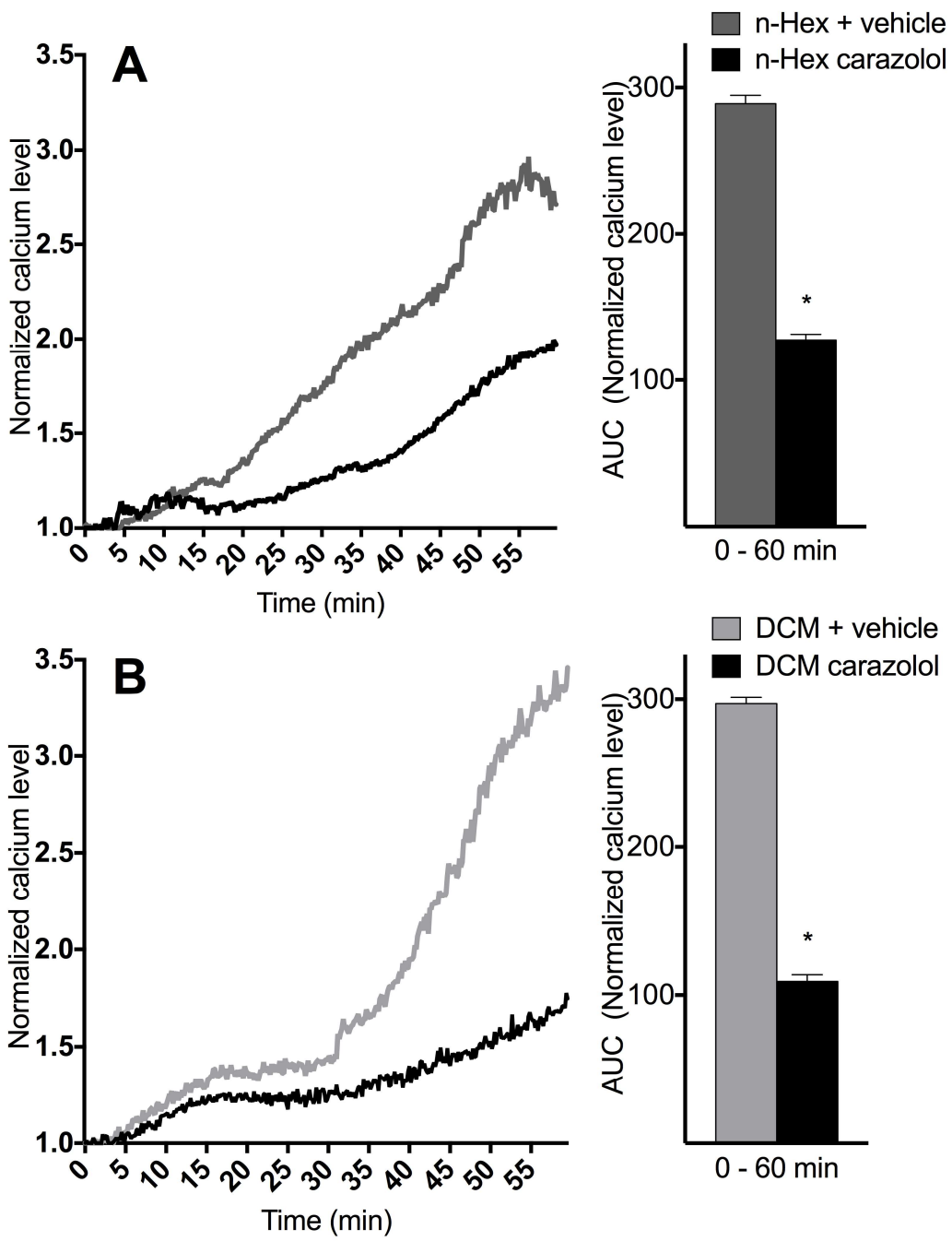

675

676 FIGURE 2

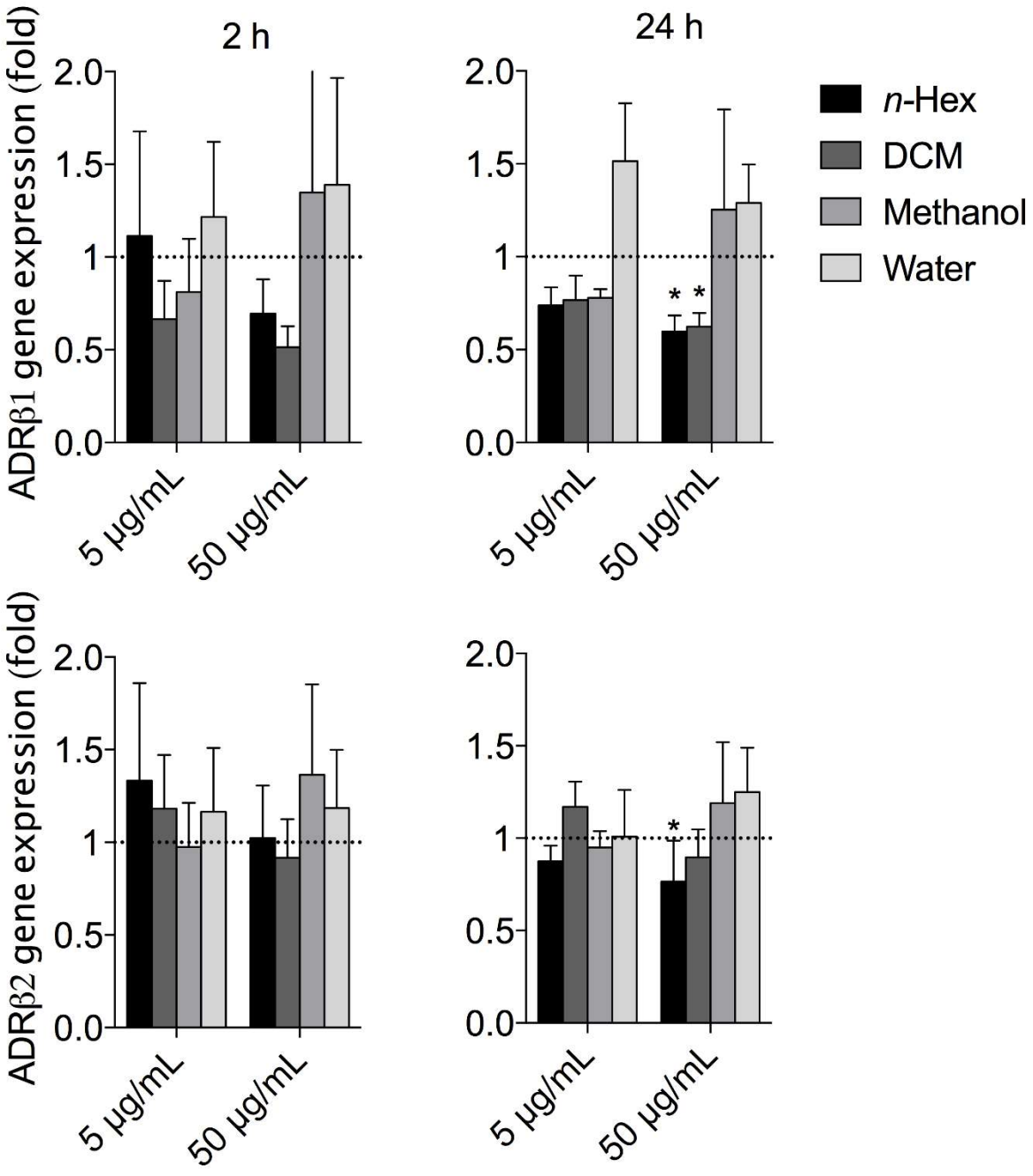

677

678

679 FIGURE 3

680

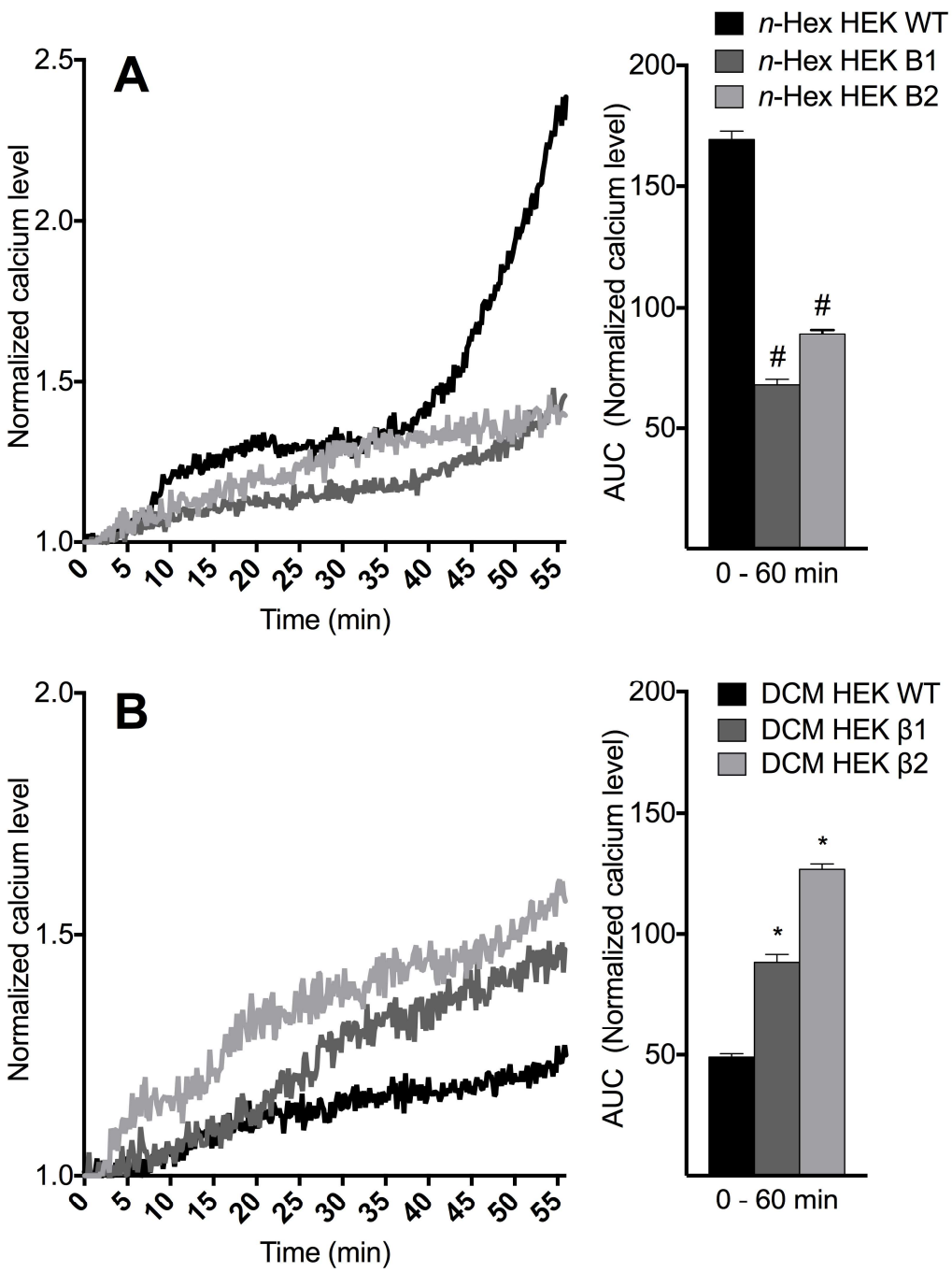

681

682 FIGURE 4.

683

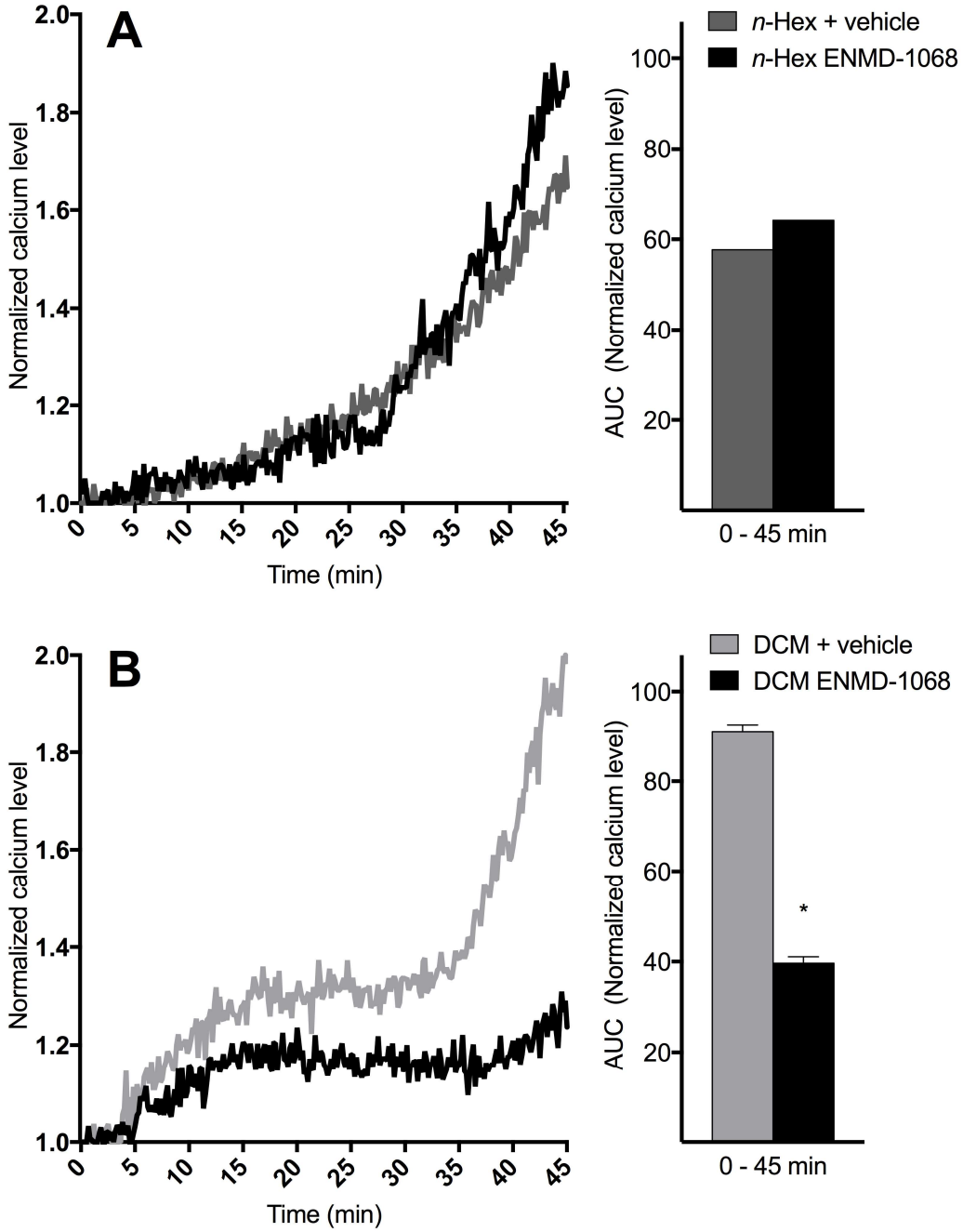

684

685 FIGURE 5

686

687

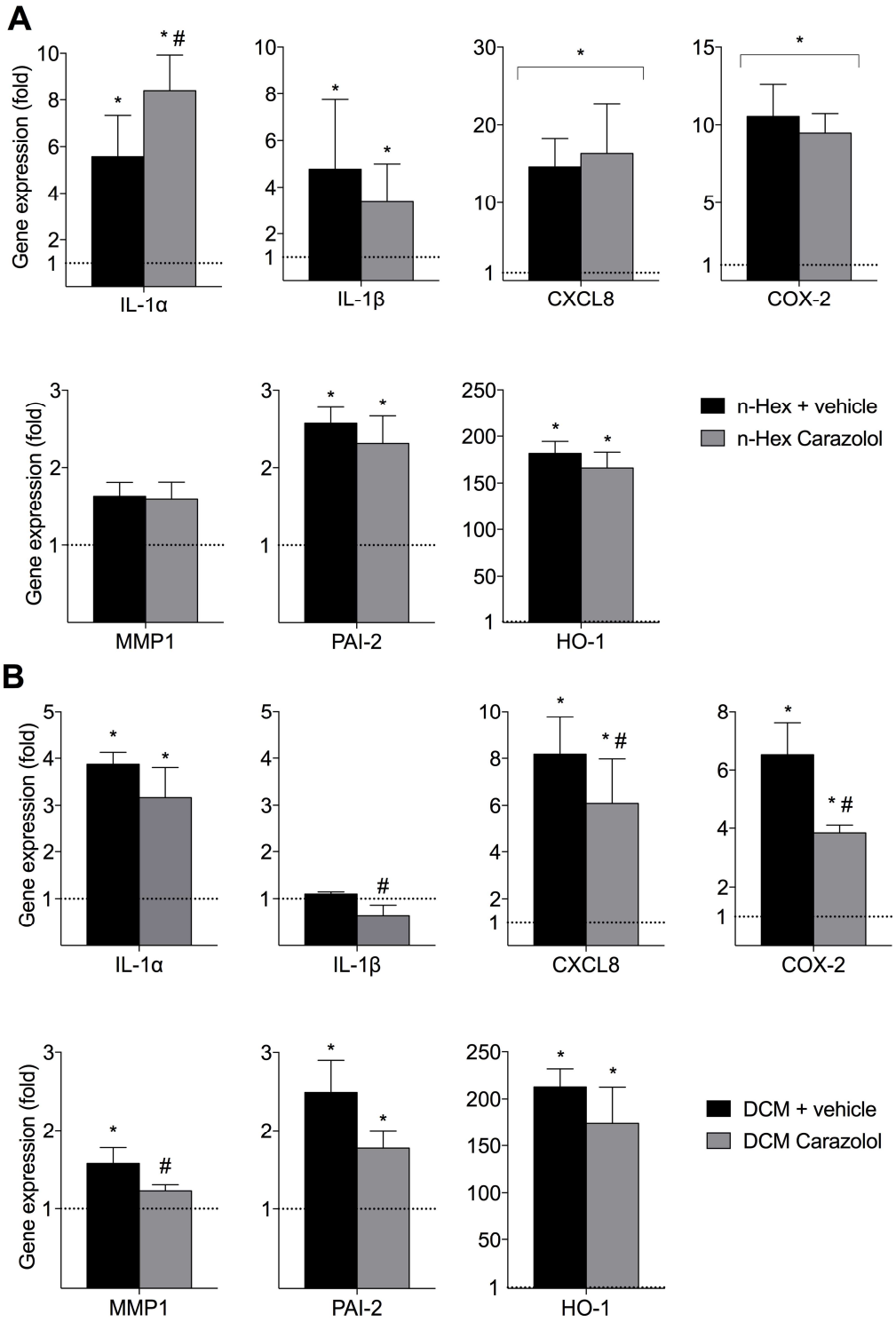
A
Gene expression (fold)
IL-1α
IL-1β
CXCL8
COX-2
MMP1
PAI-2
HO-1
n-Hex + vehicle
n-Hex Carazolol
B
DCM + vehicle
DCM Carazolol

FIGURE 6

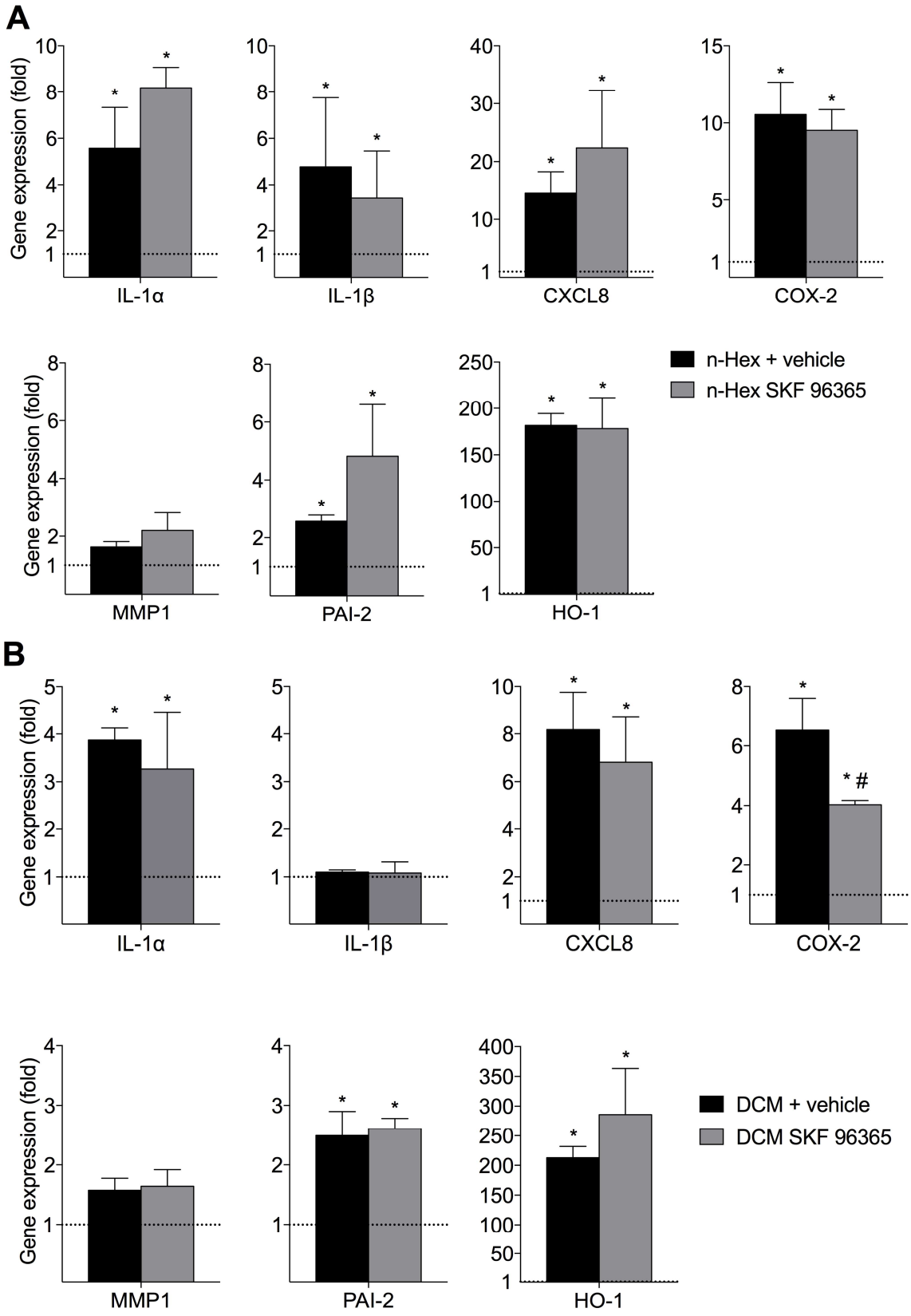

691

692 FIGURE 7